A Journal of the Gesellschaft Deutscher Chemiker

Angewandte International Edition GDCh Chemie

www.angewandte.org

Accepted Article

Title: Single-molecule determination of the isomers of D-glucose and D-fructose that bind to boronic acids

Authors: William Jamieson Ramsay and Hagan Bayley

To be cited as: *Angew. Chem. Int. Ed.* 10.1002/anie.201712740
Angew. Chem. 10.1002/ange.201712740

Link to VoR: http://dx.doi.org/10.1002/anie.201712740
http://dx.doi.org/10.1002/ange.201712740

WILEY-VCH

10.1002/anie.201712740

WILEY-VCH

Single-molecule determination of the isomers of D-glucose and D-fructose that bind to boronic acids

William J. Ramsay and Hagan Bayley*[a]

Abstract: Monosaccharides, such as D-glucose and D-fructose, exist in aqueous solution as an equilibrium mixture of cyclic isomers and can be detected with boronic acids by the reversible formation of boronate esters. The engineering of accurate, discriminating and continuous monitoring devices relies on knowledge of which cyclic isomer of a sugar binds to a boronic acid receptor. Here, by monitoring fluctuations in ionic current, we show that an engineered α-hemolysin (αHL) nanopore modified with a boronic acid reacts reversibly with D-glucose as the pyranose isomer (α-D-glucopyranose) and D-fructose as either the furanose (β-D-fructofuranose) or the pyranose (β-D fructopyranose). Both of these binding modes contradict current binding models. With this knowledge, we distinguished the individual sugars in a mixture of D-maltose, D-glucose and D-fructose.

The reversible, covalent interactions of boronic acids with diols under aqueous conditions[1] have become a lynchpin in the development of receptors for sensing biologically important 1,2-diols,[2] including saccharides.[3] For example, boronic acid-containing hydrogels have been used recently for biocompatible continuous glucose monitoring.[4] Despite the growing number of sophisticated boronic acid-based chemosensors that can detect and discriminate sugars,[5] knowledge of the structural interactions between saccharides and boronic acids remains limited.

In aqueous solution, monosaccharides such as D-fructose and D-glucose exist as mixtures of pyranose and furanose isomers, 6- and 5-membered rings, each with an α- and β-anomer. Due to the *syn*-periplanar pair of hydroxyl groups present in the glucose isomer α-D-glucofuranose, which is in an optimal orientation for boronic acid binding, it is generally accepted that this isomer binds to the boronic acid, despite making up <1% of the total composition in solution at equilibrium.[3a, 6] Similarly, the fructose isomer β-D-fructofuranose, which has ideal *syn* hydroxyl groups and is present as ~25% of the isomer population in solution,[7] is the proposed binding isomer. The stronger binding affinity of D-fructose to boronic acids over D-glucose has been attributed to the higher fraction of the optimal binding isomer in solution.[3a] However, ensemble NMR measurements[8] that attempt to characterize sugar-boronic acid interactions are hampered by the complexity of the mixture of isomers that form.

Single-molecule approaches to chemical reaction analysis provide information that is hidden or not accessible when ensembles are studied. In the nanoreactor approach, small molecule analytes form covalent bonds with a single sensing group that has been engineered onto the wall of a modified protein pore. Individual bond-making and bond-breaking events are tracked by monitoring the change in ionic current flowing through the nanoreactor, often an α-hemolysin (αHL) protein pore.[9] By this means, a variety of aqueous, reversible covalent reactions have been resolved with single-molecule resolution, including the formation and cleavage of disulfide bonds,[10] the creation and inversion of chiral centers,[11] in a multicomponent network,[12] and the continuous, stochastic motion of a small-molecule walker.[13] Here, we show that the nanoreactor approach can be used to observe the reversible reaction between a boronic acid and diol. This has enabled us to determine the isomeric structures of sugars that bind to a boronic acid from equilibrium mixtures.

The nanoreactor used here was an αHL heteroheptamer consisting of one copy of the single-cysteine mutant T117C and six copies of the wild-type (WT) protein $(WT)_6(T117C)_1$ (referred to as P_C, Figure 1a) (Section 1.2 in the Supporting Information). The presence of only one cysteine residue in the β barrel of the P_C pore allowed a single boronic acid group to be introduced into the nanoreactor for single-molecule diol detection. Maleimide **1** (3-(maleimide)phenylboronic acid) (Figure S2 in the Supporting Information) was reacted with the Cys side-chain at position 117 to form a thioether adduct (Figure 1b). When **1** entered the β barrel of P_C from the *trans* compartment, at pH 7.0 in 2 M KCl under an applied potential of −50 mV, a step decrease in the negative current was observed, after a delay, which was attributed to the formation of the adduct, P_B: $\Delta I = +4.7 \pm 0.3$ pA (number of experiments $n = 20$), over the unreacted pore current of -77 ± 2 pA ($n = 20$) (Figure S3). **1** did not react with WT_7 pores (Figure S4).

The ability of the P_B pore to sense individual diol molecules was first examined with 1,2-dihydroxybenzene (catechol) (Figure 1b). The addition of catechol to the *trans* compartment resulted in the fluctuation of the ionic current between two discrete levels separated by $\Delta I = +3.1 \pm 0.1$ pA (Figure 1c), where ΔI is the difference between the current carried by the pore with bound catechol (level 2) and that of the unoccupied pore (level 1). The events associated with catechol were not seen with unmodified $(WT)_6(T117C)_1$ pores (Figure S5). We also did not observe binding events when phenol was added to P_B from the *trans* compartment (Figure S6), suggesting two hydroxyl groups are necessary to form an adduct. In a kinetic analysis of the binding events of catechol to P_B, we assigned level 2 to the boronate ester complex and assumed that the catechol concentration inside the pore equals that in solution;[9] nanopore confinement[14] in the αHL pore has little effect (<10-fold) on the rates of reactions of uncharged small molecules.[9] The reciprocal of the mean inter-event interval (τ_{on}) is proportional to the catechol concentration, which is consistent with a bimolecular interaction for which $1/\tau_{on} = k_{on}$[catechol]. In contrast, a plot of the reciprocal of the mean lifetime of the complex (τ_{off}) versus the catechol concentration has a near zero slope, which is consistent with a unimolecular dissociation mechanism ($1/\tau_{off} = k_{off}$) (Figure 1d). The values of τ_{on} and τ_{off} were determined by fitting dwell-time histograms for each catechol concentration to

[a] Dr. W. J. Ramsay, Prof. H. Bayley
Department of Chemistry
University of Oxford
Oxford OX1 3TA
E-mail: hagan.bayley@chem.ox.ac.uk

Supporting information for this article is given via a link at the end of the document.

single exponential functions. The forward and reverse rate constants derived from the τ values (Table 1) yield an equilibrium association constant of catechol to the boronic acid of K_a = 2.4 ± 0.2 × 10^3 M^{-1} at 21 ± 1 °C (n = 3), consistent with literature values.[5] Short, spike events of varying amplitudes observed in the baseline of single-channel recordings with a P_B pore (Figure S6), which can be seen in addition to the dominant binding events of catechol in Figure 1c, were attributed to intrinsic fluctuations within the pore and were neglected during analysis.

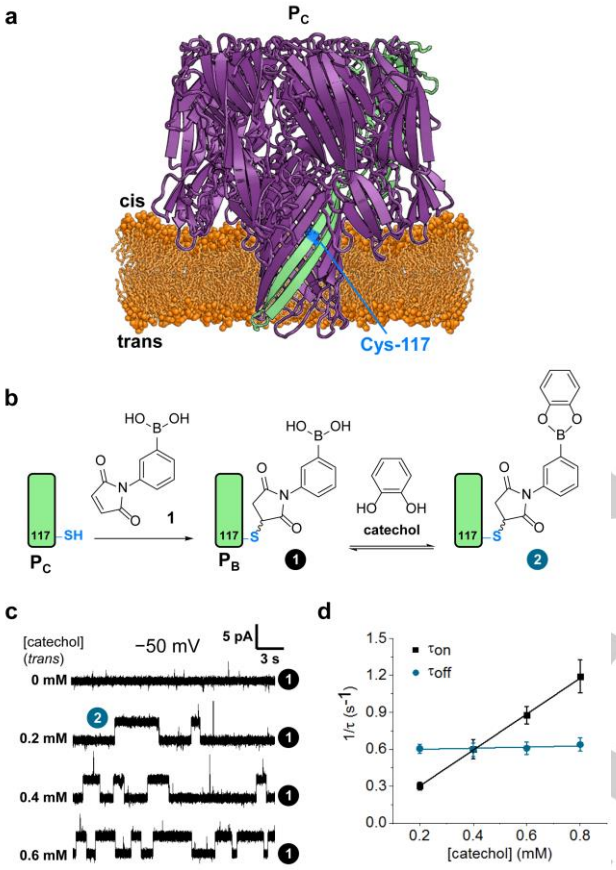

Figure 1. a) Ribbon representation of the P_C pore in a lipid bilayer. P_C contains a single Cys residue (blue) at position 117 in one of the seven subunits (green). b) Reaction of the thiol in P_C (Cys-117) with **1** to irreversibly form a thioether adduct by a Michael addition. The modified pore (P_B) reversibly forms boronate esters with catechol. c) Single-channel recordings at −50 mV with 2 M KCl, 10 mM MOPS (pH 7.0) in both compartments, and 0 to 0.6 mM catechol in the *trans* compartment. The two current levels correspond to the unoccupied pore (1) and to the state with catechol attached to the boronic acid (2). d) Plots of the reciprocals of the mean inter-event intervals (τ_{on}) and the dwell times of catechol (τ_{off}) versus the catechol concentration.

We also observed binding of D-glucose to the P_B pore (Figure 2a). Similarly to catechol, the addition of D-glucose to the *trans* compartment resulted in reversible current blockades (ΔI = +8.1 ± 0.6 pA) with a short mean life-time (5.2 ± 0.3 ms); again, P_C pores without the boronic acid sensor did not bind D-glucose (Figure S7). The association rates show a first-order dependence on the concentration of D-glucose (Figure S8), while dissociation is independent of the concentration, indicating a bimolecular interaction between D-glucose and the boronic acid; the binding affinity (K_a) of 1.5 ± 0.1 × 10^{-1} M^{-1} was weak (Table 1). Although D-glucose exists in solution as an equilibrium mixture between pyranose and furanose cyclic isomers, both with α- and β-anomers (Figure 2g), single-molecule analysis of the binding events of D-glucose suggested that one isomer was reacting with the boronic acid sensor as only one dissociation rate constant was observed. To identify this isomer, we compared the single-molecule binding data of D-glucose to other sugars and diols with known conformations in solution.

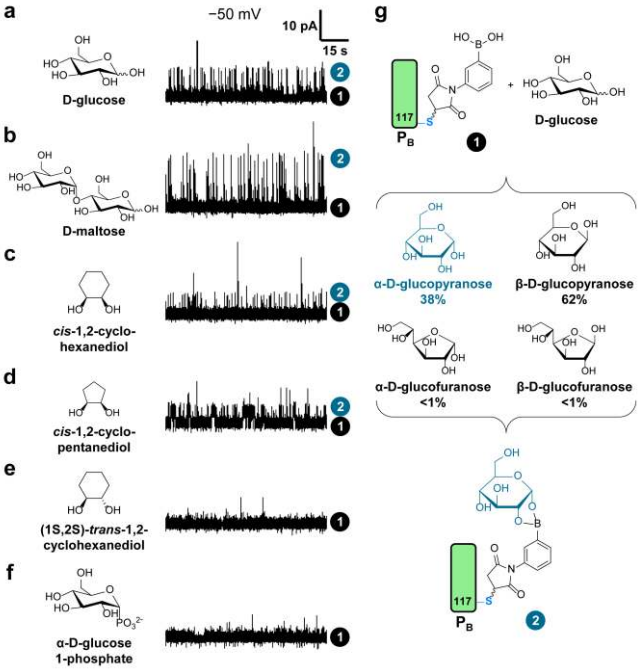

Figure 2. Single-channel recordings for various diols, added to the *trans* compartment (a – f). All traces are displayed on the same scale. Concentration of diols: (a – c, e, f) 12 mM; (d) 8 mM. Conditions: applied potential −50 mV; buffer: 2 M KCl, 100 mM MOPS (pH 7.0) in both chambers. g) Scheme showing the binding of the α-D-glucopyranose isomer (cyan) to the P_B pore from an equilibrium mixture. The percentages of each isomer in the population are shown.[6]

The addition of D-maltose, a disaccharide of two glucose units, to the P_B pore resulted in reversible current blockades (15.6 ± 0.7 pA) with twice the amplitude of the blockades recorded with D-glucose (Figure 2b, S10). The mean life-time of the events (5.2 ± 0.6 ms) and the affinity of D-maltose (K_a = 1.3 ± 0.2 × 10^{-1} M^{-1}) were nearly identical to the values for D-glucose (Table 1). As the two glucose units in D-maltose are in the pyranose form,[15] and k_{off} for the dissociation of D-maltose and D-glucose are the same, it is likely that a pyranose isomer of D-glucose binds to the boronic acid. Further support for this argument was provided by comparing the binding kinetics of D-glucose to *cis*-1,2,-cyclohexanediol (Figure 2c, S12) and *cis*-1,2-cyclopentanediol (Figure 2d, S14), which can be regarded as model compounds for pyranose and furanose binding, respectively. The rigid cyclopentane ring fixes the adjacent hydroxyl groups on one side of the ring, whereas the

conformational flexibility of cyclohexane allows limited movement of the *cis* hydroxyls. We found that the 6-membered ring diol bound to the boronic acid with k_{off} (118 ± 9 s^{-1}) and K_a (2.9 ± 0.4 × 10^{-1} M^{-1}) values similar to those of D-glucose and D-maltose (Table 1), consistent with our assignment of the binding forms of these sugars as the pyranose isomers. Further, the k_{off} of the 5-membered ring diol (2.40 ± 0.09 s^{-1}) was nearly two orders of magnitude lower than that of D-glucose and this diol bound with a much stronger affinity (K_a = 2.7 ± 0.1 × 10^1 M^{-1}) (Table 1); we suggest that the 5-membered ring diol forms a more stable boronate ester than the 6-membered ring diol, thus giving rise to the longer life-time. Therefore, our results indicate that D-glucose binds to a boronic acid as the pyranose isomer, and not as the furanose isomer as currently proposed.[3a]

We also found that the orientation of the hydroxyl groups in the 1,2-cyclohexane and 1,2-cyclopentane diols was critical for binding to the boronic acid. The addition of (1S,2S)-*trans*-1,2-cyclohexanediol (Figure 2e, S15) or (±)-*trans*-1,2-cyclopentanediol (Figure S16), in which the hydroxyl groups point in opposite directions with respect to the plane of the cycloalkane, did not result in fluctuations of the ionic current during electrical recordings. These results, in combination with the binding events observed with *cis*-1,2-cyclohexanediol, suggested that only 1,2-hydroxyl groups positioned on the same side of a cyclohexane ring (*cis*) bind to a boronic acid. Because the D-glucose pyranose anomer α-D-glucopyranose has 1,2-hydroxyl groups positioned *cis* at C_1 and C_2, and β-D-glucopyranose has hydroxyl groups at C_1 through C_4 positioned *trans* to each other (Figure 2g), our results suggest that α-D-glucopyranose binds to a boronic acid through the *cis*-hydroxyl groups at C_1 and C_2. This proposition was further supported by the lack of interaction of α-D-glucose 1-phosphate with the P_B pore (Figure 2f, S17), consistent with previous reports that did not report binding of this phosphorylated sugar to a fluorinated boronic acid-appended pyridinium salt receptor.[5]

Table 1. Kinetic constants for the formation of complexes between the P_B pore and diol.

Diol	Amplitude Block (pA)[a]	k_{on} ($M^{-1}s^{-1}$)	k_{off} (s^{-1})	K_a (M^{-1})[b]
catechol[c]	3.1 ± 0.1	1460 ± 20	0.61 ± 0.05	2.4 ± 0.2 × 10^3
D-glucose[d]	8.1 ± 0.6	29.8 ± 0.5	193 ± 13	1.5 ± 0.1 × 10^{-1}
D-maltose[d]	15.6 ± 0.7	24 ± 1	191 ± 22	1.3 ± 0.2 × 10^{-1}
cis-1,2-cyclohexane-diol[d]	5.3 ± 0.3	34 ± 3	118 ± 9	2.9 ± 0.4 × 10^{-1}
cis-1,2-cyclopentane-diol[d]	3.6 ± 0.1	65 ± 2	2.40 ± 0.09	2.7 ± 0.1 × 10^1

[a] The errors were obtained from the fitting of a dwell-time histogram to the binding events. [b] Calculated by using $K_a = k_{on}/k_{off}$. [c] 2 M KCl, 10 mM MOPS, Chelex, pH 7.0, recorded at −50 mV and 21 ± 1 °C. [d] 2 M KCl, 100 mM MOPS, Chelex, pH 7.0, recorded at −50 mV and 21 ± 1 °C.

We next examined the binding of D-fructose to the P_B pore (Figure 3, S19). Similar to the binding of D-glucose, the addition of D-fructose to the *trans* compartment resulted in reversible current blockades (ΔI = +7.5 ± 0.3 pA) (Figure 3a). However, the dwell-time histogram of the current blockades, which was obtained from idealized current traces by using QuB software (QUB 2.0, University at Buffalo), was well fitted by a two-component probability density function that yielded mean dwell-times of 143 ± 8 ms and 4762 ± 454 ms[16] (Figure 3b). This indicated that two different isomers in the equilibrium mixture of D-fructose were stochastically binding to the boronic acid. The nearly two orders of magnitude difference in the mean dwell-times was similar to the difference observed between the pyranose (*cis*-1,2-cyclohexanediol) and furanose (*cis*-1,2-cyclopentanediol) model compounds, and therefore we initially assigned the shorter dwell-time to the binding of β-D-fructopyranose (68% of the total isomer population in solution), which has been characterized with X-ray crystallography,[17] and the longer dwell-time to the binding of β-D-fructofuranose (22%) (Figure 3c). The ratio of the calculated uncorrected k_{on} values for β-D-fructopyranose (43 ± 2 $M^{-1}s^{-1}$) and β-D-fructofuranose (18.2 ± 0.4 $M^{-1}s^{-1}$) reflected the proposed isomer fractions in solution[7] (Figure S20). Although α-D-fructopyranose has *syn* hydroxyl groups at C_4 and C_5 ideal for binding to the boronic acid (Figure 2c), our single-molecule analysis is not able to detect an isomer with a low population (here 3%), especially if, as is likely, its binding events are similar in amplitude and duration to those of the dominant β-D-fructopyranose (68%).

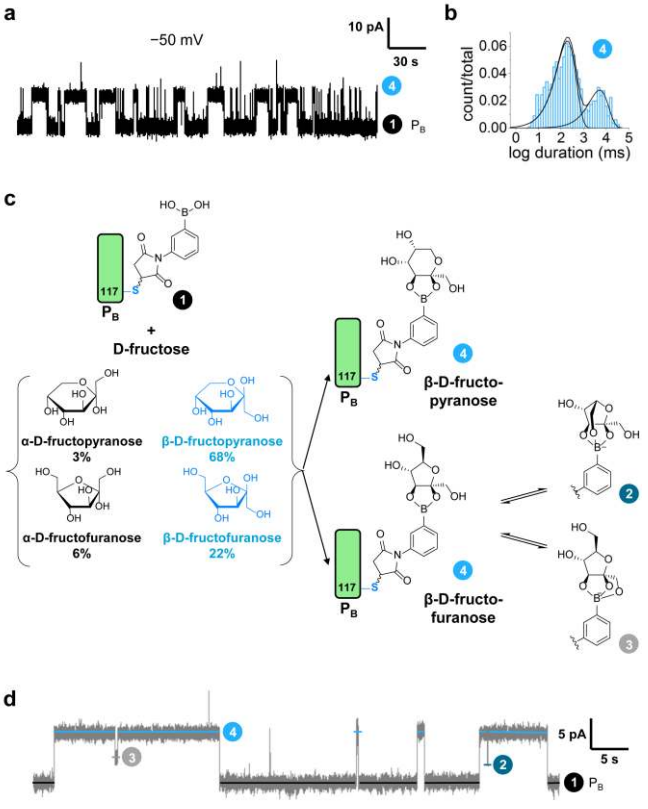

Figure 3. a) Representative current recording from a P_B pore at −50 mV with 8 mM D-fructose in the *trans* compartment (conditions: 2 M KCl, 100 mM MOPS, pH 7.0, 21 ± 1 °C). b) Dwell-time histogram of the current blockades (level 4,

blue) fitted with a two-component probability density function. c) Proposed scheme describing the binding of the β-D-fructopyranose and β-D-fructofuranose isomers from an equilibrium mixture to the P_B pore (the percentages of each isomer in the mixture are shown).[7] d) Further analysis of the current recordings during the reaction identified additional events accessed from level 4, which were assigned as level 3 (grey) and level 2 (cyan).

Further analysis of the blockade level (assigned as level 4, Figure 3d) with the longer life-time (4762 ± 454 ms), which is attributed to the binding of β-D-fructofuranose, showed that two additional levels (ΔI = +5.4 ± 0.4 pA and +3.4 ± 0.5 pA, assigned as levels 3 and 2, respectively) were derived from level 4. Levels 3 and 2 were accessed only from level 4, and always returned to level 4; transitions between levels 3 and 2 were not observed. We constructed a four-state model to describe the observed transitions (Figure S20). The associated rate constants were determined by analyzing idealized current traces with Hidden Markov modelling (QUB 2.0, University at Buffalo). The association rates for D-fructose (describing the transition from level 1 to level 4), comprising the rates k_{14}(β-D-fructopyranose) and k_{14}(β-D-fructofuranose), both showed a first-order dependence on the concentration of D-fructose, while dissociation (rates k_{41}(β-D-fructopyranose) and k_{41}(β-D-fructofuranose)) were independent of the concentration, consistent with bimolecular interactions between β-D-fructopyranose and P_B and between β-D-fructofuranose and P_B. The transitions between levels 4 (β-D-fructofuranose) and 3 (k_{43} and k_{34}) and between levels 4 (β-D-fructofuranose) and 2 (k_{42} and k_{24}) were concentration independent, suggesting that level 2 and level 3 arose from rearrangement of the sugar complex bound to the boronic acid. Because we assigned level 4 to the adduct between P_B and β-D-fructofuranose (bound *via* the *cis*-diol pair at C_2 and C_3), we postulated that level 3 and level 2 arose from additional coordination of the hydroxyl groups at C_1 and C_6, respectively, to from an anionic tetrahedral boron complex[1b] (Figure 3c). In support of this argument, we observed that D-fructose 1,6-bisphosphate, in which the hydroxyl groups at C_1 and C_6 are replaced with non-coordinating phosphate groups, bound to P_B with only one blockade level (Figure S21). In addition, we also observed only two different current blockades when D-fructose 6-phosphate bound to P_B (Figure S22), consistent with the initial binding of the *cis* hydroxyl groups at C_2 and C_3 to the boronic acid, followed by the intramolecular coordination of the hydroxyl group at C_1 (but not C_6, which is phosphorylated). The assignment of level 3 to the four-coordinate binding species with β-D-fructofuranose (Figure 3c) was based on the similar blockade level observed with D-fructose 6-phosphate.

To demonstrate the potential of P_B as a saccharide sensor, the discrimination of the components of solutions of different sugars was accomplished by analyzing the current blockade amplitudes and mean dwell-times (Figure 4, S23). The components in a mixture of D-maltose (30 mM) and D-glucose (30 mM) were readily distinguished by visual inspection of a current recording (Figure 4a). In a 2D event-distribution plot of current block *versus* log(dwell-times), two clearly separated populations were apparent based on differences in the amplitudes of current block (Figure 4b), although the dwell-times of the sugars were the same. A mixture of D-fructose (15 mM), D-glucose (30 mM) and D-maltose (30 mM) was also analyzed (Figure 4c). The binding events of the disaccharide (D-maltose) were easily identified and separated from the binding events of the monosaccharides (D-fructose and D-glucose) by analyzing the blockade amplitudes (Figure 4d). Although the two monosaccharides gave indistinguishable blockade levels, the identity of D-glucose and D-fructose could be distinguished by dwell-time analysis (Figure 4e). The short dwell time of α-D-glucopyranose bound to the boronic acid was separated from the two longer dwell-times of β-D-fructopyranose and β-D-fructofuranose.

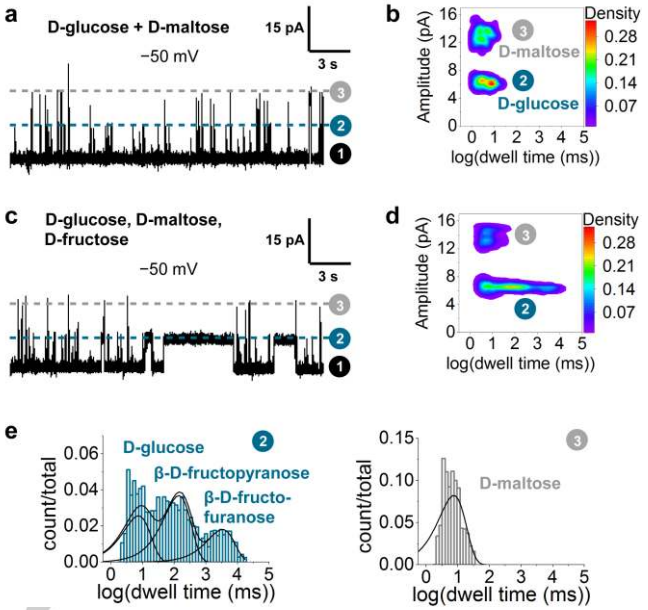

Figure 4. a) Single-channel recording at −50 mV with D-glucose (30 mM) (level 2, cyan) and D-maltose (30 mM) (level 3, grey) in the *trans* compartment. b) 2D event-distribution plot displaying the extent of current block *versus* log(event duration). c) Single-channel recording with a mixture of D-fructose (15 mM), D-glucose (30 mM) and D-maltose (30 mM) in the *trans* compartment. d) 2D event-distribution plot displaying current block *versus* log(event duration) for a mixture of three sugars. D-maltose (level 3) was first discriminated from the monosaccharides (level 2) by analyzing the extents of current block. e) D-glucose and D-fructose were identified by analyzing the dwell times. Histograms were fitted with one- or three component probability density functions. All measurements were performed in 2 M KCl, 100 mM MOPS, pH 7.0, 21 ± 1 °C.

In this study, we have shown that single-molecule analysis of reversible, covalent interactions with an engineered protein nanopore identifies which cyclic isomers of D-glucose and D-fructose bind to a boronic acid in solution. The approach can also identify and discriminate the components of sugar mixtures. We anticipate that this new binding information will impact the design of more accurate continuous glucose monitoring devices for medical diagnostics.[18]

Acknowledgements

This work was supported by a European Research Council Advanced Grant.

Keywords: single-molecule • α-hemolysin • nanoreactor • boronic acid • sugar detection

[1] a) Z. Guo, I. Shin, J. Yoon, *Chem. Comm.* **2012**, *48*, 5956-5967; b) S. D. Bull, M. G. Davidson, J. M. H. van den Elsen, J. S. Fossey, A. T. A. Jenkins, Y.-B. Jiang, Y. Kubo, F. Marken, K. Sakurai, J. Zhao, T. D. James, *Acc. Chem. Res.* **2013**, *46*, 312-326.

[2] a) J. Yoon, A. W. Czarnik, *Bioorg. & Med. Chem.* **1993**, *1*, 267-271; b) K. E. Secor, T. E. Glass, *Org. Lett.* **2004**, *6*, 3727-3730; c) A. E. Hargrove, R. N. Reyes, I. Riddington, E. V. Anslyn, J. L. Sessler, *Org. Lett.* **2010**, *12*, 4804-4807.

[3] a) X. Wu, Z. Li, X.-X. Chen, J. S. Fossey, T. D. James, Y.-B. Jiang, *Chem. Soc. Rev.* **2013**, *42*, 8032-8048; b) B. M. Chapin, P. Metola, S. L. Vankayala, H. L. Woodcock, T. J. Mooibroek, V. M. Lynch, J. D. Larkin, E. V. Anslyn, *J. Am. Chem. Soc.* **2017**, *139*, 5568-5578.

[4] a) Q. Dou, D. Hu, H. Gao, Y. Zhang, A. K. Yetisen, H. Butt, J. Wang, G. Nie, Q. Dai, *RSC Adv.* **2017**, *7*, 41384-41390; b) C. Zhang, M. D. Losego, P. V. Braun, *Chem. Mat.* **2013**, *25*, 3239-3250; c) S. Gamsey, J. T. Suri, R. A. Wessling, B. Singaram, *Langmuir* **2006**, *22*, 9067-9074.

[5] J. Axthelm, S. H. C. Askes, M. Elstner, U. R. G, H. Görls, P. Bellstedt, A. Schiller, *J. Am. Chem. Soc.* **2017**, *139*, 11413-11420.

[6] R. Polacek, J. Stenger, U. Kaatze, *J. Chem. Phys.* **2002**, *116*, 2973-2982.

[7] T. Barclay, M. Ginic-Markovic, M. R. Johnston, P. Cooper, N. Petrovsky, *Carbohydr. Res.* **2012**, *347*, 136-141.

[8] a) J. C. Norrild, H. Eggert, *J. Am. Chem. Soc.* **1995**, *117*, 1479-1484; b) J. C. Norrild, H. Eggert, *J. Chem. Soc., Perkin Trans. 2* **1996**, 2583-2588.

[9] H. Bayley, T. Luchian, S. H. Shin, M. B. Steffensen in *Single Molecules and Nanotechnology* (Eds.: R. Rigler, H. Vogel), Springer, **2008**, pp. 251-277.

[10] T. Luchian, S.-H. Shin, H. Bayley, *Angew. Chem. Int. Ed.* **2003**, *42*, 3766-3771.

[11] S.-H. Shin, M. B. Steffensen, T. D. W. Claridge, H. Bayley, *Angew. Chem. Int. Ed.* **2007**, *46*, 7412-7416.

[12] M. B. Steffensen, D. Rotem, H. Bayley, *Nat. Chem.* **2014**, *6*, 603.

[13] G. S. Pulcu, E. Mikhailova, L.-S. Choi, H. Bayley, *Nat. Nanotech.* **2014**, *10*, 76.

[14] Y. Lin, Y.-L. Ying, Y.-T. Long, *Current Opinion in Electrochemistry* **2018**, *7*, 172-178.

[15] D. E. Levy, P. Fügedi in *The Organic Chemistry of Sugars*, CRC Press, **2005**.

[16] N. Ni, S. Laughlin, Y. Wang, Y. Feng, Y. Zheng, B. Wang, *Bioorg. & Med. Chem.* **2012**, *20*, 2957-2961.

[17] S. P. Draffin, P. J. Duggan, G. D. Fallon, *Acta Cryst. E* **2004**, *60*, o1520-o1522.

[18] a) I. R. Scorei in *Breast Cancer - Current and Alternative Therapeutic Modalities* (Ed.: E. Gunduz), InTech, **2011**, pp. 91-114; b) S. Jin, Y. Cheng, S. Reid, M. Li, B. Wang, *Med. Res. Rev.* **2010**, *30*, 171-257; c) X. Sun, T. D. James, *Chem. Rev.* **2015**, *115*, 8001-8037.

10.1002/anie.201712740

WILEY-VCH

COMMUNICATION

Sweet reaction: The aqueous, reversible covalent chemistry of boronic acids and diols can be monitored inside a protein nanoreactor. The approach is used to identify which cyclic isomers of D-glucose and D-fructose bind to a boronic acid in aqueous solution. Both of these binding modes contradict current binding models.

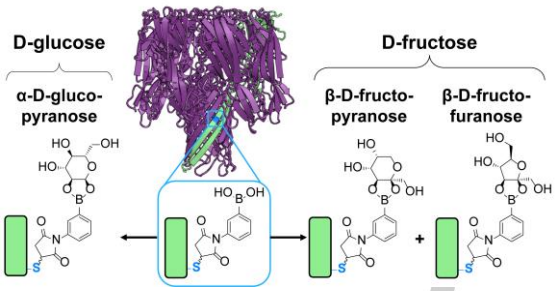

*William J. Ramsay and Hagan Bayley**

Page No. – Page No.

Single-molecule determination of the isomers of D-glucose and D-fructose that bind to boronic acids